

Discovery of a Potent, Long-Acting, and CNS-Active Inhibitor (BIA 10-2474) of Fatty Acid Amide Hydrolase

László E. Kiss,^{*[a]} Alexandre Beliaev,^[a] Humberto S. Ferreira,^[a] Carla P. Rosa,^[a] Maria João Bonifácio,^[b] Ana I. Loureiro,^[b] Nuno M. Pires,^[b] P. Nuno Palma,^[b] and Patrício Soares-da-Silva^[b, c]

Fatty acid amide hydrolase (FAAH) can be targeted for the treatment of pain associated with various medical conditions. Herein we report the design and synthesis of a novel series of heterocyclic-*N*-carboxamide FAAH inhibitors that have a good alignment of potency, metabolic stability and selectivity for FAAH over monoacylglycerol lipase (MAGL) and carboxylesterases (CEs). Lead optimization efforts carried out with benzotria-

zoyl- and imidazolyl-*N*-carboxamide series led to the discovery of clinical candidate **8I** (3-(1-(cyclohexyl(methyl)carbamoyl)-1*H*-imidazol-4-yl)pyridine 1-oxide; BIA 10-2474) as a potent and long-acting inhibitor of FAAH. However, during a Phase I clinical trial with compound **8I**, unexpected and unpredictable serious neurological adverse events occurred, affecting five healthy volunteers, including the death of one subject.

Introduction

Fatty acid amide hydrolase (FAAH, EC 3.5.1.99), an integral membrane-bound enzyme, is a member of the extensive family of serine hydrolases referred to as the amidase signature (AS) family.^[1] It catalyzes the degradation of lipid signaling fatty acid amides including the sleep-inducing oleamide and endogenous cannabinoid anandamide (AEA).^[2] AEA binds and activates both central (CB₁) and peripheral (CB₂) cannabinoid receptors of the endocannabinoid system (ECS).^[3] The modulation of AEA levels via inhibition of FAAH has potential clinical relevance in a wide range of diseases and pathological conditions. Therefore, both the ECS and FAAH have become recognized as promising therapeutic targets for the treatment of a range of central and peripheral disorders.^[4–5] Importantly, phenotypes observed in FAAH knockout mice allowed researchers

to expect the efficiency of FAAH inhibitors to avoid being compromised by the typical side effects of direct CB₁ agonists.^[6] Due to increasing interest over the last two decades, numerous small-molecule inhibitors of FAAH belonging to various chemical classes have been reported (see recent reviews^[5–10] and references cited therein).

The X-ray crystal structure of the rat catalytically active transmembrane domain deleted FAAH was first unveiled in 2002, in complex with an irreversible inhibitor (methoxyarachidonoyl fluorophosphonate (MAFP)).^[11] Later on, an engineered “humanized” rat (h/r)FAAH was produced by interconverting the active site residues of rat and human FAAH, using site-directed mutagenesis.^[12] This h/rFAAH combined the efficient rFAAH recombinant expression with the inhibitor sensitivity profile of hFAAH, thus greatly facilitating the design of new inhibitors. Since then, a number of inhibitors have been co-crystallized with this form of the enzyme.^[12–19]

The most important classes of compounds with different mechanism of action are the reversible inhibitor heterocyclic ketones^[20] exemplified by **1** (OL-135), and the irreversible covalently binding inhibitors such as carbamates^[21] (e.g., **2** (URB597)) and ureas^[13] (e.g., **3** (PF3845)) (Figure 1). Interestingly, despite the rather high chemical stability of the urea functional group in **3**, FAAH is yet inhibited in an irreversible manner by covalently modifying the enzyme’s active site.^[22] Of the urea class^[22–24] the most interesting compounds to have been advanced into clinical trials are **4** (JNJ-42165279)^[25] developed by Johnson & Johnson and **5** (PF-04457845)^[26] by Pfizer (Figure 1). Unfortunately, the clinical development of **4** and **5** have been suspended as a precautionary measure following serious safety issues with **8I** (BIA 10-2474) and due to lack of therapeutic effect,^[27] respectively. Recent efforts from Merck led to the discovery of oxazole **6** (MK-4409)^[28] which has also advanced into clinical development. Compound **6** is described

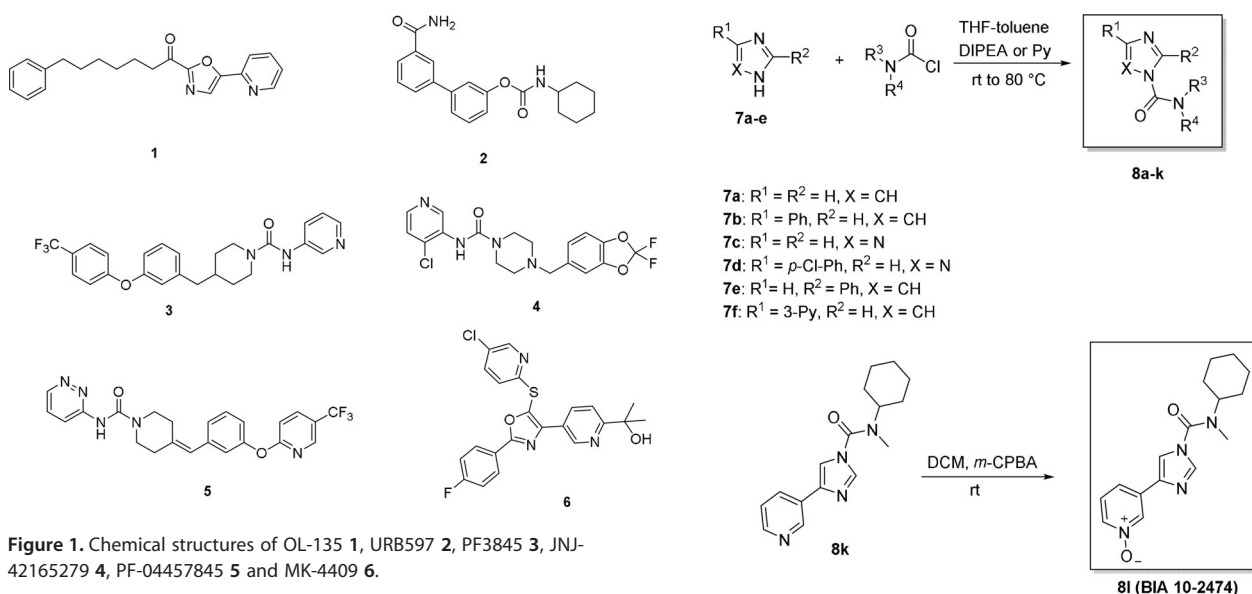
[a] Dr. L. E. Kiss, Dr. A. Beliaev, Dr. H. S. Ferreira, Dr. C. P. Rosa
Laboratory of Chemistry, Department of Research and Development, BIAL-Portela & C^o, S.A., À Avenida da Siderurgia Nacional, 4745-457 Coronado (S. Romão and S. Mamede) (Portugal)
E-mail: laszlo.kiss@bial.com

[b] Dr. M. J. Bonifácio, Dr. A. I. Loureiro, Dr. N. M. Pires, Dr. P. N. Palma, Dr. P. Soares-da-Silva
Laboratory of Pharmacology, Department of Research and Development, BIAL-Portela & C^o, S.A., À Avenida da Siderurgia Nacional, 4745-457 Coronado (S. Romão and S. Mamede) (Portugal)

[c] Dr. P. Soares-da-Silva
MedInUp-Center for Drug Discovery and Innovative Medicines, University of Porto, Praça Gomes Teixeira, 4099-002 Porto (Portugal)

Supporting information and the ORCID identification number(s) for the author(s) of this article can be found under:
<https://doi.org/10.1002/cmdc.201800393>.

© 2018 The Authors. Published by Wiley-VCH Verlag GmbH & Co. KGaA. This is an open access article under the terms of the Creative Commons Attribution-NonCommercial-NoDerivs License, which permits use and distribution in any medium, provided the original work is properly cited, the use is non-commercial and no modifications or adaptations are made.



as a reversible FAAH inhibitor, but there are no clinical results published at this point.

Our group set out to design a fast-onset, long-acting and CNS-active FAAH inhibitor, which may be useful for the treatment of pain associated with various medical conditions. Preliminary screening of selected compounds sourced from both commercial vendors and those selected from our in-house collections for FAAH inhibition led to the identification of imidazole **8a** (Figure 2, *N*-methyl-*N*-phenyl-1*H*-imidazole-1-carboxamide), which showed moderate *in vitro* activity (88% inhibition at a concentration of 10 μM in rat brain homogenates).

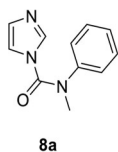


Figure 2. Chemical structure of screening hit **8a**.

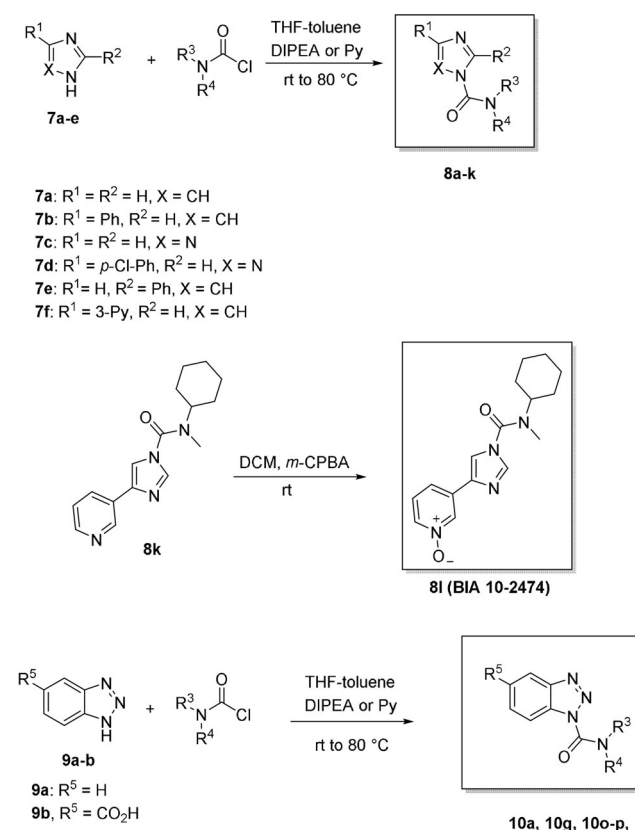
At that time, compound **8a** represented a novel scaffold^[29] in the field of FAAH inhibitors, although during our research program a patent application filed by an academic group independently disclosed similar heterocyclic-*N*-carboxamide scaffolds, claiming them as dual inhibitors of monoacylglycerol lipase (MAGL) and FAAH.^[30] The structure of **8a** was deemed to be readily amenable to the exploration of structure–activity relationships (SAR), and it was therefore selected as the starting point for a medicinal chemistry program.

Herein we describe a novel series of potent *in vivo* CNS-active benzotriazolyl- and imidazolyl-*N*-carboxamides that were designed and synthesized in our laboratory, including **8l** (BIA 10-2474), which in January 2016 faced a severe incident in a Phase I clinical trial, where one person died and others suffered adverse neurological effects.

Results and Discussion

Chemistry

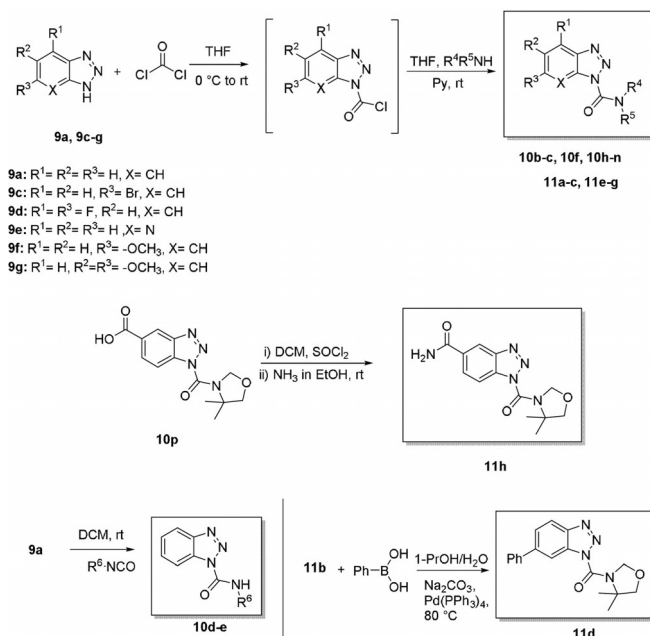
The synthetic routes used to obtain the initial heterocyclic-*N*-carboxamide inhibitors are outlined in Scheme 1. The necessa-



Scheme 1. Preparation of imidazole and benzotriazole analogues.

ry dialkylcarbamoyl chloride intermediates were obtained either from commercial sources or prepared by a published method.^[31] The target heterocyclic-*N*-carboxamides were synthesized under two different conditions. More reactive heterocycles such as **7a–d** and **7f** were smoothly carbamoylated with dialkylcarbamoyl chlorides in THF at reflux containing base (*N,N*-diisopropylethylamine (DIPEA) or pyridine) to provide the target compounds **8a,b**, **8d**, and **8f–k** in moderate yields. The 3-pyridyl imidazole analogue **8k** was further oxidized to pyridine *N*-oxide **8l** (BIA 10-2474) on reaction with *meta*-chloroperbenzoic acid (*m*CPBA) in dichloromethane at room temperature. Due to reduced reactivity of **7e** and **9a,b** different reaction conditions were applied for preparing compounds **8c**, **10a**, **10g**, and **10o,p**, wherein **7e** and **9a,b** were deprotonated with sodium hydride in THF at 0 °C followed by reaction with the corresponding dialkylcarbamoyl chlorides to give phenyl imidazole **8c** and benzotriazoles **10a**, **10g**, and **10o,p** in fairly good yields.

The general synthetic routes to support SAR exploration within the series of *N*-benzotriazolyl carboxamide derivatives are depicted in Scheme 2. Benzotriazoles **9a** and **9c–g** were acylated with 20% toluenic solution of phosgene in THF. Benzotriazole-*N*-carbonyl chloride intermediates thus obtained were treated with secondary amines in THF using pyridine as base to provide the desired *N,N*-disubstituted benzotriazole carboxamides (**10b,c**, **10f**, **10h–n**, **11a–c**, **11e–g**) in moderate yield. The carboxamide derivative **11h** was prepared from carboxylic acid intermediate **10p**. Activation of **10p** with thionyl



Scheme 2. Preparation of benzotriazole analogues.

chloride (SOCl₂) afforded the corresponding acyl chloride intermediate, which was subsequently reacted with ethanolic ammonia solution to provide **11h**. Mono-substituted benzotriazole *N*-carboxamides **10d,e** were obtained by treating benzotriazole **9a** with isocyanates in CH₂Cl₂ at room temperature. Construction of the biphenyl ring in **11d** was accomplished via Suzuki coupling. 6-Bromobenzimidazole **9b** was smoothly converted into **11d** upon reaction with phenylboronic acid in a mixture of 1-propanol/water using palladium catalyst (Pd(PPh₃)₄) and sodium carbonate as base.

Pharmacology

In vitro screening of all new compounds was carried out in rat brain membranes. FAAH activity was determined by measuring the formation of [³H]ethanolamine using tritium-labeled AEA as described previously.^[32] In the first phase of our hit-to-lead optimization program, modification by substitution or replacement of the imidazole ring in **8a** with other common heterocycles were investigated. To facilitate the interpretation of the SAR, all prepared analogues shared the same *N*-methylaniline moiety on the right-hand side of the molecule and were evaluated at two different concentrations. The results for a representative selection of compounds are provided in Table 1 and reported in residual enzymatic activity.

Whilst the initial screening hit **8a** exhibited fairly promising activity at a concentration of 10 μM, it was found to be completely inactive at 100-fold lower concentration. The 4-phenyl derivative **8b** displayed slightly increased inhibition over the parent **8a**, whereas shifting the phenyl ring to the C2 position of the imidazole ring (**8c**) led to drastic decrease in FAAH inhibition. Within the series of heterocycles with three heteroatoms, the unsubstituted 1,2,4-triazole **8d** was found to possess

Table 1. In vitro FAAH inhibition by selected heterocyclic *N*-carboxamide analogues in rat brain homogenates.

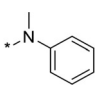
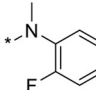
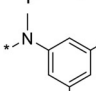
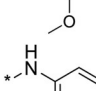
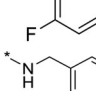
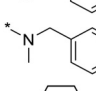
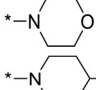
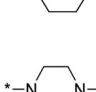
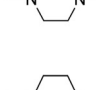
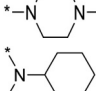
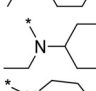
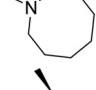
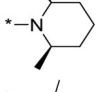
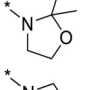
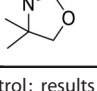
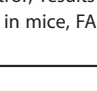
Compd	HetAr	10 μM ^[a]	0.1 μM ^[a]
8a		12 ± 3	112 ± 20
8b		0 ± 0	84 ± 7
8c		93 ± 6	115 ± 37
8d		0 ± 0	17 ± 2
8e		0 ± 0	61 ± 5
10a		0 ± 0	1 ± 0

[a] Percent of control; results are means ± SD (n=4), determined in rat brain homogenates after 15 min pre-incubation time.

enhanced inhibition over the screening hit **8a**. Inclusion of a *p*-chlorophenyl group at the 3-position of the imidazole ring (**8e**) made little difference in potency relative to imidazole analogue **8b**. However, it was then discovered that in vitro inhibition could markedly be enhanced by condensing the triazole core in **8d** with phenyl ring (**10a**). Benzotriazole **10a** was clearly the most potent inhibitor with an IC₅₀ value of 7 nM, and therefore, it was further studied pharmacologically. Target selectivity of **10a** for FAAH relative to CEs and MAGL was evaluated in vitro in rat liver microsomes and in rat cerebellum cytosol, respectively. Inhibitor **10a** showed significant selectivity for FAAH (IC₅₀ = 7 nM) over CE (IC₅₀ > 1 μM) and MAGL (IC₅₀ > 100 μM), although it inhibited CEs to a greater extent than reference compounds **2** and **3** (Table 2).

In another experiment, **2**, **3**, and **10a** were assessed for in vivo FAAH inhibition. Compounds were orally administered to overnight-fasted mice at a dose of 30 mg kg⁻¹, and thereafter at 1 h post-administration the FAAH activity was determined. As shown in Table 2, whilst **2** and **3** exhibited over 90% inhibition in both the liver and brain, compound **10a** only moderately inhibited FAAH both centrally and peripherally. At this point compound **10a** was selected as an early lead for further optimization. The SAR around our lead structure **10a** was investigated by varying the amino side chain of the carboxamide core structure. Accordingly, we proceeded to synthesize a restricted series of benzotriazoles (**10b-d**) aimed at enhancing in vitro efficacy whilst maintaining good target selectivity over CEs and MAGL. Introduction of electron-withdrawing groups (EWGs) such as fluorine in the aromatic ring (**10b**) had no ben-

Table 2. In vitro FAAH, CE, MAGL, and in vivo FAAH inhibition by selected benzotriazole *N*-carboxamides.

Compd	HetAr	100 nM ^[a,b]		10 nM ^[a,b]		Liver ^[a,c]	Brain ^[a,c]	CEs ^[a,d]	MAGL ^[a,e]
		100 nM ^[a,b]	10 nM ^[a,b]	100 nM ^[a,b]	10 nM ^[a,b]				
2		0 ± 0	15 ± 3	6 ± 1	9 ± 2	72 ± 5	87 ± 4		
3		7 ± 4	101 ± 31	2 ± 2	1 ± 0	95 ± 17	87 ± 12		
10a		1 ± 0	42 ± 12	34 ± 5	34 ± 9	31 ± 2	73 ± 4		
10b		2 ± 1	35 ± 3	ND	ND	40 ± 1	70 ± 6		
10c		76 ± 0	ND	ND	ND	ND	ND		
10d		100 ± 5	ND	ND	ND	ND	ND		
10e		2 ± 1	13 ± 1	84 ± 6	87 ± 7	67 ± 4	4 ± 1		
10f		0 ± 0	0 ± 0	6 ± 2	1 ± 0	24 ± 1	2 ± 2		
10g		3 ± 0	39 ± 10	41 ± 5	47 ± 2	33 ± 2	10 ± 2		
10h		0 ± 0	0 ± 0	6 ± 1	8 ± 1	24 ± 2	7 ± 5		
10i		0 ± 0	0 ± 0	15 ± 4	20 ± 5	27 ± 1	7 ± 4		
10j		0 ± 0	1 ± 0	30 ± 5	88 ± 7	28 ± 2	12 ± 4		
10k		1 ± 2	1 ± 0	1 ± 0	0 ± 0	30 ± 1	73 ± 3		
10l		94 ± 12	ND	ND	ND	57 ± 7	80 ± 18		
10m		15 ± 1	62 ± 6	ND	ND	30 ± 2	58 ± 6		
10n		71 ± 7	ND	ND	ND	28 ± 1	35 ± 5		
10o		17 ± 3	71 ± 2	ND	ND	60 ± 7	84 ± 25		
11a		2 ± 1	78 ± 25	2 ± 1	0 ± 0	81 ± 6	90 ± 5		

[a] Percent of control; results are means ± SD ($n=4$); ND: not determined. [b] Determined in rat brain homogenates after 15 min pre-incubation time. [c] 30 mg kg⁻¹ p.o. in mice, FAAH activity was determined 1 h after administration. [d] $C_{inhib} = 10 \mu\text{M}$ in rat liver microsomes. [e] $C_{inhib} = 100 \mu\text{M}$ in rat cerebellum cytosol.

eficial effect on in vitro inhibitory potency. Increasing the electron density on the aromatic ring in **10a** by appropriate substitution at the *meta* positions led to a weakly active compound

(**10c**). Removal of the *N*-methyl group in **10b** completely abolished FAAH inhibition (**10d**). Moreover, compounds **10b–d** inhibited CE and MAGL to an appreciable extent. The next round

of SAR concentrated on analogues that incorporate benzylic, cycloaliphatic, and saturated heterocyclic side chains (**10e–k**). Compounds **10e–k** were evaluated both in vitro (FAAH, CEs, and MAGL) and in vivo (30 mg kg⁻¹, p.o., mice 1 h post-dose). Despite the promising in vitro FAAH activity of the *N*-benzyl derivative **10e**, only residual in vivo inhibition was observed both centrally and peripherally. In contrast, the *N*-methyl-*N*-benzyl derivative **10f**, also highly potent in vitro, showed evidence of in vivo efficacy, but it was uninteresting in terms of selectivity.

Morpholine **10g** exhibited weaker inhibitory activity than **10f** both in vitro and in vivo without improving target selectivity. The piperidine **10h** and piperazine analogues **10i,j** exhibited higher in vitro inhibition than either **2** or **3** at a concentration of 10 nM, irrespective of the type of substitution. Unfortunately, both CEs and MAGL were inhibited by **10h–j** to a high extent. The in vivo efficacy of **10h–j** both centrally and peripherally was similar to that of **2** and **3**, with the exception of **10j**, which showed a clear preference for peripheral FAAH. Another effort within the benzotriazole *N*-carboxamide series focused on further functionalization of the amino moiety. We envisioned that compounds endowed with higher steric hindrance in the region of the carbonyl group might improve the poor target selectivity of earlier *N,N*-dialkyl analogues (**10f–j**) without compromising the excellent in vitro and good in vivo FAAH inhibitory activity. Indeed, this hypothesis was borne out, as the *N*-methyl-*N*-cyclohexyl derivative **10k**, highly potent in vitro, exhibited greater in vivo efficacy over **10f–j** with considerably improved selectivity over MAGL. Thus, compound **10k** exhibited the greatest promise at this point, and subsequent efforts focused on this particular *N*-alkyl, *N*-cycloalkyl series, leading to the elaboration of derivatives **10l–n** shown in the lower half of Table 2. Elongation of the *N*-methyl group of **10k** with a methylene spacer resulted in inactive derivative **10l**. Incorporation of eight-membered (**10m**) macrocyclic amines was less tolerated in vitro without providing an improvement in selectivity over both MAGL and CEs. A structural isomer of **10m**, which includes two methyl groups at the 2- and 6-positions of the piperidine ring (**10n**), was weakly potent in vitro. However, the five-membered 2,2-dimethyloxazolidine analogue **10o**, which displayed moderate in vitro FAAH inhibition, was found to be endowed with better target selectivity than any other previously synthesized analogue. Moving the two methyl groups to the 4-position of the oxazolidine ring to change the steric bulk around the carbonyl group provided **11a**. This compound had slightly higher in vitro FAAH inhibition and improved target selectivity over regioisomer **10o**, but more importantly, demonstrated potent oral activity. On the basis of these findings, **11a** was selected for further pharmacological studies. The IC₅₀ value of **11a** was calculated to be 19 nM. The dose-dependent central and peripheral inhibitory ability of **11a** was assessed in mouse (1 h post-dose) given increasing doses of compound **11a** (0.001–3.0 mg kg⁻¹, p.o.). Compound **11a** was found to inhibit both peripheral and cerebral FAAH with ED₅₀ values of 7 and 61 μg kg⁻¹, respectively.

Reference compound **3** was a slightly weaker inhibitor of FAAH in the liver than **11a** under the same conditions, but in

Table 3. In vitro CYP450 metabolic stability of **11a**, **11h**, **8h**, and **8l** in various species.

Compd	Mouse ^[a]	Rat ^[a]	Dog ^[a]	Primate ^[a]	Human ^[a]
11a	5 ± 0	26 ± 0	1 ± 0	0 ± 0	52 ± 9
11h	87 ± 9	87 ± 0	101 ± 6	57 ± 3	96 ± 8
8h	62 ± 0	88 ± 6	54 ± 0	41 ± 3	75 ± 4
8l	99 ± 2	91 ± 1	94 ± 2	88 ± 1	95 ± 1

[a] C_{inhib} = 5 μM in liver microsomes after 1 h incubation; data are given in percent of remaining, and are means ± SD (n = 4).

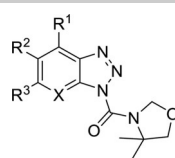
the brain was found to be equipotent (ED_{50(liver)} = 23 μg kg⁻¹; ED_{50(brain)} = 63 μg kg⁻¹). In another experiment, inhibitor **11a** was incubated with liver microsomes (at 5 μM) prepared from different species to evaluate the potential likelihood of metabolic instability. Moderate to high metabolism was observed in different species with the highest degradation observed in mouse, primates, and dog (Table 3).

Despite the outstanding in vivo efficacy, benzotriazole derivative **11a** was not considered for further development, but it was selected for additional optimization to improve its pharmacological profile. Blocking the 4,4-dimethyloxazolidinyl moiety in structure of **11a**, further investigations into the effect of the aromatic substitution on stability against CYP450 activity (50 μM, 1 h incubation) and in vivo efficacy (0.1 mg kg⁻¹, mouse, p.o., 8 h post-dose) were carried out. Table 4 lists the results for new compounds and includes comparative data for compounds **2** and **3**. Despite the high in vitro potency of **2** (IC₅₀ = 5 nM),^[33] only residual in vivo FAAH inhibition was observed in both liver and brain (0.1 mg kg⁻¹, mouse, p.o., 8 h post-dose). In contrast, compound **11a** displayed similar in vivo potency to that of **3** in both liver and brain. Inclusion of a bromine atom at C6 of the benzotriazole ring provided a metabolically unstable compound (**11b**) and made little difference in the in vivo inhibitory profile. The 4,6-difluoro derivative **11c** did not perform better in vivo than the monobromo derivative **11b** and failed to improve metabolic stability. Incorporation of a bulky phenyl group as in **11d** was found to be detrimental for in vivo potency.

Replacement of the phenyl ring in **11a** with a pyridyl ring gave **11e**, which demonstrated over 85% peripheral and cerebral inhibition with a slight increase in inhibition of CEs. As expected, methoxy derivative **11f** was poorly active in vivo, most probably due to extensive CYP450-mediated metabolism. Surprisingly, the 5,6-dimethoxy derivative **11g** was endowed with reasonably good metabolic stability and displayed impressive FAAH inhibition, although it is a good inhibitor of MAGL. Finally, the optimal compound from this series was achieved by simple incorporation of a carboxamide group at C5 of **11a** to produce compound **11h** with high CNS efficacy and good CYP450 stability in vitro over **11a** in various species (Table 3).

For completeness of the SAR, we considered replacement of the benzotriazole ring in **11h** with other heterocycles such as imidazole and triazole. We were interested to see what sort of pharmacological effect in terms of in vivo efficacy and target selectivity could be expected by this modification. From the early imidazole and triazole inhibitors (Table 1) the latter class

Table 4. In vivo FAAH and in vitro CE and MAGL inhibition data of selected benzotriazole *N*-carboxamides.

Compd						Liver ^[a,b]	Brain ^[a,b]	CEs (10 μM) ^[a,c]	MAGL (100 μM) ^[a,d]	CYPs (50 μM) ^[e]
	R ¹	R ²	R ³	X						
2						74 ± 20	91 ± 7	72 ± 5	87 ± 4	ND
3						7 ± 4	5 ± 1	95 ± 17	87 ± 12	ND
11a	H	H	H	CH		10 ± 4	24 ± 7	81 ± 6	90 ± 5	25 ± 2
11b	H	H	Br	CH		16 ± 6	77 ± 29	73 ± 9	67 ± 12	8 ± 2
11c	F	H	F	CH		19 ± 9	71 ± 10	82 ± 5	68 ± 3	8 ± 1
11d	H	H	Ph	CH		54 ± 6	76 ± 18	92 ± 2	77 ± 4 ^[f]	73 ± 2
11e	H	H	H	N		14 ± 7	12 ± 4	61 ± 11	72 ± 5	ND
11f	H	H	OCH ₃	CH		39 ± 7	125 ± 38	79 ± 13	96 ± 1 ^[f]	0 ± 0
11g	H	OCH ₃	OCH ₃	CH		8 ± 4	9 ± 3	72 ± 5	7 ± 1	55 ± 0
11h	H	CONH ₂	H	CH		6 ± 1	6 ± 1	81 ± 7	96 ± 2	67 ± 2

[a] Percent of control; results are means ± SD *n* = 4. [b] 0.1 mg kg⁻¹ p.o. in mice, FAAH activity was determined 8 h after administration. [c] In rat liver microsomes. [d] C_{inhib} = 100 μM in rat cerebellum cytosol. [e] C_{inhib} = 50 μM in mouse liver microsomes after 1 h incubation, data are given in percentage remaining, and are means ± SD (*n* = 4). [f] C_{inhib} = 12.5 μM.

was ruled out due to poor selectivity over CEs. Imidazole **8b** was devoid of CE inhibition, and despite the lower in vitro potency, it was endowed with more enhanced in vivo inhibition (30 mg kg⁻¹, mouse, p.o., 1 h post-dose) both centrally and peripherally over our initial benzotriazole derivative **10a** (Table 5). Therefore, we were encouraged to synthesize further imidazole analogues (**8f,g**) for in vitro and in vivo comparison with their benzotriazole counterparts (**10i**, **10j**, and **11a**). Compounds that exhibited over 90% of control in the MAGL and CE assays were evaluated in vivo in mice (0.1 mg kg⁻¹, p.o., 8 h post-dose), and the results are listed in Table 5. The majority of the newly synthesized compounds were much less efficacious in vitro than their benzotriazole analogues. Compound **8f**, the analogue of **11a**, demonstrated some degree of peripheral inhibition, but was ineffective centrally. Although piperazine analogue **8g** fully abolished FAAH activity at a concentration of 100 nM, it inhibited both CEs and MAGL somewhat. Increasing the steric hindrance near the carbonyl group led to a more selective compound **8h**, which exhibited over 90% in vivo FAAH inhibition in the brain and liver. Replacement of the *N*-benzyl group (**8h**) with an oxygen atom (**8i**) or methylene group (**8j**) led to a decrease in central inhibition. The more polar and basic pyridyl analogue **8k** failed to improve in vivo efficacy in the brain over the parent **8j**. However, the even more polar pyridine *N*-oxide derivative **8l** displayed impressive inhibition in both brain and liver with no measurable effect in vitro in CE and MAGL assays. Furthermore, compound **8l** displayed favorable in vitro metabolic stability in various species (Table 3). Generally, we can say that within the imidazole scaffold few correlations could be established between the results of in vitro and in vivo FAAH activity. Possible explanations include in vivo accumulation of the inhibitors, which has not been observed (manuscript in preparation), or their interaction with the enzyme might be affected by the enzyme environment in vitro (brain membranes) or in vivo; further studies are required to understand this effect.

Having identified **11h**, **8h**, and **8l** from these series as having excellent in vivo FAAH inhibitory activity (>90% of control in brain and liver at a dose of 0.1 mg kg⁻¹, mouse, p.o.) and good selectivity over CEs and MAGL (>80% of control), subsequent experiments with **3**, **8h**, **8l**, and **11h** were designed. Figure 3 highlights their FAAH inhibition profile in

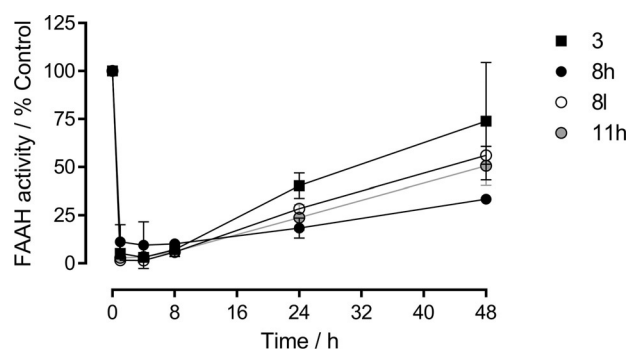
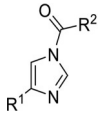
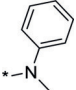
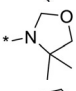
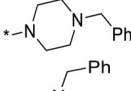
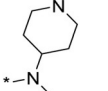
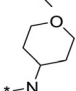
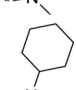
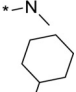
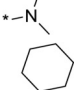


Figure 3. Liver FAAH activity after oral administration of 0.1 mg kg⁻¹ of compounds **3** (■), **8h** (●), **8l** (○) and **11h** (○) to mice. Results are means ± SD (*n* = 4).

mouse liver and brain homogenates at a dose of 0.1 mg kg⁻¹, p.o. Compounds **3**, **8h**, **8l**, and **11h** were found to achieve their maximum inhibitory effect at 1 h post-dose in the liver. Thereafter, the constant peripheral inhibition of FAAH (>90%) was sustained over the next 7 h, followed by a gradual return to lower levels at later time points.

The profile of central inhibition by **3**, **8h**, and **8l** was found to be different from that of their liver inhibition. Inhibitors **3**, **8h**, and **8l** produced their maximal inhibitory effect (>90%) in the brain only at 8 h post-dose, and significant central inhibition by **8h** and **8l** (>50%) was maintained up to 48 h post-administration (Figure 4). In contrast, compound **11h** displayed

Table 5. In vivo FAAH and in vitro CE and MAGL inhibition data of selected imidazole *N*-carboxamides.

Compd	R ¹	R ²					
			100 nM ^[a,b]	Liver ^[a,c]	Brain ^[a,c]	CEs (10 μM) ^[a,d]	MAGL (100 μM) ^[a,e]
8b	Ph		84 ± 7	11 ± 5 ^[f]	14 ± 17 ^[f]	105 ± 5	ND
8f	Ph		94 ± 10	53 ± 6	92 ± 7	95 ± 6	92 ± 3
8g	Ph		1 ± 0	ND	ND	52 ± 2	61 ± 6
8h	Ph		41 ± 7	10 ± 2	11 ± 4	97 ± 8	92 ± 8
8i	Ph		104 ± 18	12 ± 4	38 ± 18	96 ± 7	96 ± 1
8j	Ph		37 ± 3	33 ± 2	86 ± 5	90 ± 11	91 ± 3
8k	3-Py		75 ± 7	13 ± 4	75 ± 16	97 ± 3	94 ± 4
8l	3-Py- <i>N</i> -oxide		85 ± 11	6 ± 2	8 ± 2	102 ± 5	96 ± 4

[a] Percent of control; results are means ± SD ($n=4$). [b] Determined in rat brain homogenates after 15 min pre-incubation time. [c] 0.1 mg kg⁻¹ p.o. in mice, FAAH activity was determined 8 h after administration. [d] In rat liver microsomes. [e] $C_{inhib} = 100 \mu\text{M}$ in rat cerebellum cytosol. [f] 30 mg kg⁻¹ p.o. in mice, FAAH activity was determined 1 h after administration.

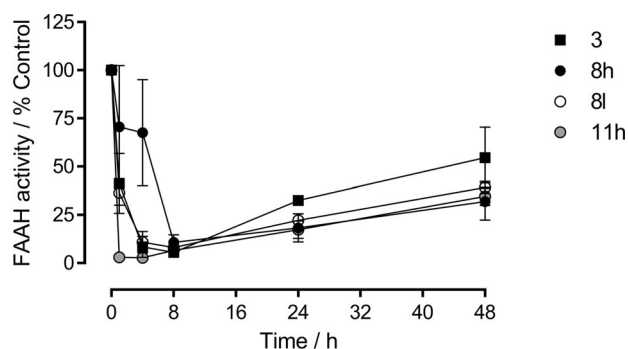


Figure 4. Brain FAAH activity after oral administration of 0.1 mg kg⁻¹ of compounds **3** (■), **8h** (●), **8l** (○) and **11h** (●) to mice. Results are means ± SD ($n=4$).

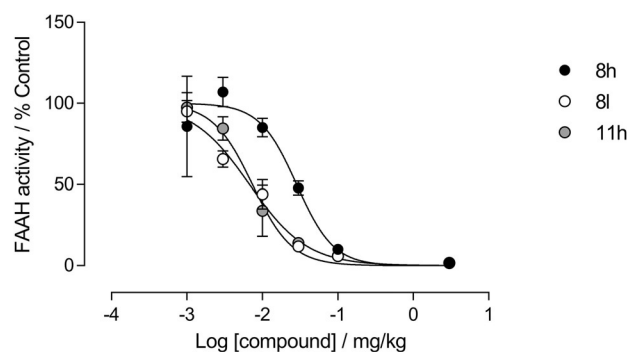


Figure 5. Effect of increasing doses of compounds **8h** (●), **8l** (○) and **11h** (●) on mice liver FAAH activity 8 h after oral administration of each compound. Results are means ± SD ($n=4$).

similar inhibitory profile ($t_{max} = 1$ h) both centrally and peripherally and was found to achieve a long-lasting effect.

Finally, we examined the dose-dependent FAAH inhibitory profiles of **8h**, **8l**, and **11h**. Mice were given increasing doses of these three compounds ranging from 0.001 to 3 mg kg⁻¹

p.o., thereafter, at 8 h post-administration the FAAH activity was assayed in liver and brain. The results (Figures 5 and 6) demonstrate that all three compounds were very efficacious in these assays.

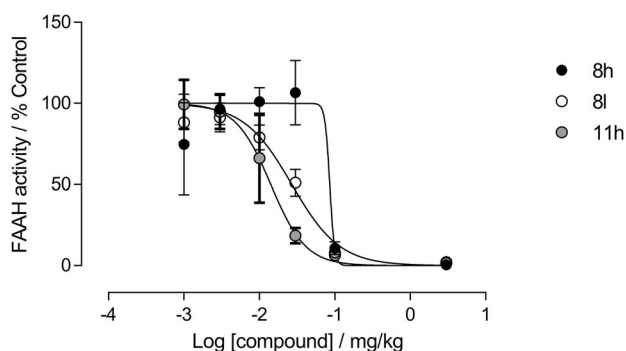


Figure 6. Effect of increasing doses of compounds **8h** (●), **8l** (○) and **11h** (●) on mice brain FAAH activity 8 h after oral administration of each compound. Results are means \pm SD ($n=4$).

In the liver compounds **8l** and **11h** are essentially equipotent, with ED_{50} values of $7 \mu\text{g kg}^{-1}$, whereas inhibitor **8h** was slightly less potent with an ED_{50} value of $28 \mu\text{g kg}^{-1}$. Again, **11h** was the most potent compound out of **8h**, **8l**, and **11h** at inhibiting cerebral FAAH with an ED_{50} value of $14 \mu\text{g kg}^{-1}$. Imidazoles **8h** and **8l** displayed less marked inhibition with ED_{50} values of approximately 79 and $27 \mu\text{g kg}^{-1}$, respectively.

The overall pharmacological profiles of **8h**, **8l**, and **11h** did not demonstrate marked differences, and all three inhibitors were efficacious in the low $\mu\text{g kg}^{-1}$ range. Therefore, other factors such as ease of large-scale manufacturing and cost of synthesis played a role in preclinical candidate selection.

Our synthetic feasibility analysis revealed difficulties in the synthesis of **11h**. Any kind of 1*H*-benzotriazole compound substituted at the 5-position is present in three tautomeric forms, which may result in different products in the carbamoylation step. Indeed, **11h** was always contaminated with the unwanted regioisomer (substituted at the 6-position of the benzotriazole ring), and isolation of a pure sample of **11h** was not feasible by simple recrystallization. In contrast, the most efficacious imidazole compound **8l** was easily prepared from inexpensive raw materials in a simple process involving few steps.^[34] Furthermore, inhibitor **8l** was screened against a panel of 97 off-targets (Caliper Life Sciences), including neurotransmitter-related targets, ion channels, prostaglandins, growth factors/hormones, peptides, and enzymes. At a concentration of $10 \mu\text{M}$, none of these off-targets were found to be inhibited/blocked by **8l** (Supporting Information). Therefore, compound **8l** was selected as a preclinical candidate and later advanced into Phase I clinical studies.

Conclusions

A novel series of potent benzotriazolyl- and imidazolyl-*N*-carboxamides were developed from an *in vitro* imidazolyl-*N*-carboxamide hit **8a**. The 4,4-dimethyloxazolidinyl derivative **11a** was the most potent compound from this series with limited *in vitro* metabolic stability in various animal species. Consequently, the carboxamide-substituted derivative **11h** was prepared and found to be highly efficacious in the CNS, metabolically stable, and devoid of off-target effects (CEs and MAGL).

Further optimization resulted in other selective (CEs and MAGL) *in vivo* potent imidazolyl *N*-carboxamides such as **8h** and **8l**. On the basis of overall pharmacological profile, inhibitor **8l** was selected for clinical development. Since the accident in the clinical trial concerning **8l** in which one person died and four were hospitalized with neurological symptoms,^[35] there has been much speculation into its cause. Investigations conducted by the French authorities concluded that it was an unexpected effect of the test item, having ruled out other extraneous causes. Their conclusion was that the accident was likely to have been caused by an unknown off-target effect of **8l**.^[36] However, the nature of this off-target effect remains obscure, although much speculation has centered around the idea that **8l** is not particularly selective for FAAH. In fact, a recent activity-based profiling of serine hydrolases revealed that **8l** inhibited not only FAAH, but ABHD6 and some other serine hydrolases, namely FAAH2, CES1, CES2, CES3, ABHD11, LIPE, and PNPLA6, albeit at concentrations several-fold higher than those needed for FAAH inhibition.^[37] Although the published data provide information about the selectivity of **8l**, they do not allow a conclusion about which of the identified off-targets could be responsible for the observed toxicity. Even in the case of PNPLA6, which has previously been linked to organophosphate-based neurotoxicity in humans, it was shown that carbamoylation of the enzyme (expected effect of **8l**) was not neuropathic.^[38] Detailed pharmacological characterization of the clinical candidate **8l** will be addressed in a separate publication including a discussion about off-target effects, in addition to the preliminary data already disclosed.^[39–41] Preliminary information concerning the safety profile of **8l** during the clinical trial BIA-102474-101 have been provided, and the conclusions drawn already revealed that: 1) following multiple ascending doses up to 20 mg, inhibitor **8l** was found to be safe and well tolerated and systemic exposure to anandamide increased in a dose-dependent manner,^[42] and 2) five out of six subjects exposed to **8l** at 50 mg day^{-1} reported unexpected serious CNS-related adverse events, for which causality cannot be excluded; the available data do not allow one to discern specific reasons that could have caused the serious adverse events, which were considered unexpected and unpredictable.^[43]

Experimental Section

Chemistry

NMR spectra were recorded on a Bruker Avance III (600 MHz) Spectrometer with solvent used as internal standard, and data are reported in the order: chemical shift (ppm), number of protons, multiplicity (s, singlet; d, doublet; dd, doublet of doublets; t, triplet; q, quartet; m, multiplet; br, broad), approximate coupling constant (J) in Hertz and assignment of a signal. Elemental analyses were performed on a CE Instruments EA 1110 CHNS analyzer. The purity of the compounds in all cases was higher than 95%. Analytical TLC was performed on pre-coated silica gel plates (Merck 60 Kieselgel F₂₅₄) and visualized with UV light. Solvents and reagents were purchased from Aldrich, Merck, and Fluka and were used without further purification.

***N*-Methyl-*N*-phenyl-1*H*-imidazole-1-carboxamide (8a).** To a stirred solution of imidazole **7a** (681 mg, 10 mmol) in THF (15 mL) at 0 °C was added a solution of methyl(phenyl)carbamic chloride (848 mg, 5 mmol) in toluene (6 mL). After being stirred for 2 h at room temperature, the reaction was filtered, and the filtrate was evaporated. Chromatography (in CH₂Cl₂) followed by trituration with Et₂O afforded **8a** as a white powder (446 mg, 44%), mp: 58 °C. ¹H NMR (CDCl₃): δ = 7.57 (1H, s), 7.39 (2H, t, *J* = 7.7 Hz), 7.32 (1H, t, *J* = 7.3 Hz), 7.13 (2H, d, *J* = 7.7 Hz), 6.85 (1H, s), 6.81 (1H, s), 3.50 ppm (3H, s); ¹³C NMR (CDCl₃): δ = 150.2, 142.9, 137.7, 130.3, 129, 128, 125.9, 118.4, 40.1 ppm; Elemental analysis calcd (%) for (C₁₁H₁₁N₃O): C 65.66, H 5.51, N 20.88, found: C 65.68, H 5.11, N 21.03.

***N*-Methyl-*N*,4-diphenyl-1*H*-imidazole-1-carboxamide (8b).** To a stirred solution of 4-phenyl-1*H*-imidazole **7b** (433 mg, 3.0 mmol) in THF (10 mL) was added DIPEA (0.78 mL, 4.5 mmol) followed by a solution of methyl(phenyl)carbamic chloride (534 mg, 3.15 mmol) in toluene (4 mL). The reaction mixture was stirred at room temperature for 1 h, then was heated at 80 °C for 1 h. After being cooled to room temperature the reaction was evaporated and partitioned between CH₂Cl₂ and water. The organic layer was separated, dried over MgSO₄, filtered and evaporated. Trituration in a mixture of petroleum ether/EtOAc (3:1) followed by filtration and drying gave **8b** as a beige powder (465 mg, 56%), mp: 104–105 °C. ¹H NMR (CDCl₃): δ = 7.60 (2H, d, *J* = 7.7 Hz), 7.53 (1H, s), 7.40 (2H, t, *J* = 7.7 Hz), 7.34 (1H, m), 7.32 (2H, t, *J* = 7.6 Hz), 7.25 (1H, m), 7.19 (2H, m), 7.18 (1H, s), 3.52 ppm (3H, s); ¹³C NMR (CDCl₃): δ = 150.1, 142.9, 141.4, 137.7, 132.8, 130.4, 128.5, 128.2, 127.4, 126, 125, 113.5, 40.2 ppm; Elemental analysis calcd (%) for (C₁₇H₁₅N₃O): C 73.63, H 5.45, N 15.15, found: C 73.25, H 5.29, N 15.05.

***N*-Methyl-*N*,2-diphenyl-1*H*-imidazole-1-carboxamide (8c).** To a stirred suspension of sodium hydride (166 mg, 4.15 mmol, 60% dispersion in mineral oil) in THF (10 mL) at 0 °C was added a solution of 2-phenyl-1*H*-imidazole **7e** (500 mg, 3.47 mmol) in THF (5 mL). The mixture was stirred at 0 °C for 30 min then was allowed to stir at room temperature for 2 h. The mixture was cooled again to 0 °C and a solution of methyl(phenyl)carbamic chloride (616 mg, 3.63 mmol) in THF (5 mL) was added dropwise. The reaction was stirred in the cold for 0.5 h, then was allowed to stir at room temperature for two days. Thereupon, water was added at 0 °C and the solvent was evaporated and then the oily residue was partitioned between CH₂Cl₂ and water. The organic phase was separated, washed with water and brine, then dried over MgSO₄, filtered and evaporated to leave an oily solid. Chromatography (petroleum ether/EtOAc, 2:1) allowed separation of the product as a pale-yellow solid (166 mg, 17%), mp: 123–125 °C. ¹H NMR (CDCl₃): δ = 7.43–7.24 (6H, m), 7.14–6.93 (4H, m), 6.33 (2H, br), 3.37 ppm (3H, sbr); ¹³C NMR (CDCl₃): δ = 151.9, 146.5, 141.4, 130.3, 129.3, 129, 128.9, 128.3, 127.3, 126.9, 124.1, 120, 38.9 ppm; Elemental analysis calcd (%) for (C₁₇H₁₅N₃O): C 73.63, H 5.45, N 15.15, found: C 73.83, H 5.74, N 14.82.

***N*-Cyclohexyl-*N*-methyl-4-(pyridin-3-yl)-1*H*-imidazole-1-carboxamide (8k).** To a stirred suspension of 3-(1*H*-imidazol-4-yl)pyridine dihydrochloride **7f** (0.654 g, 3 mmol) in THF (10 mL) was added potassium *tert*-butoxide (0.673 g, 6.00 mmol) and the mixture was held at reflux for 1 h. Then, *N,N*-dimethylformamide (1 mL) was added, and heating was continued for an additional 30 min. The resultant brown suspension was cooled to room temperature and treated with pyridine (0.37 mL, 4.50 mmol) and *N,N*-dimethylpyridin-4-amine (0.037 g, 0.300 mmol) followed by addition of cyclohexyl(methyl)carbamic chloride (0.553 g, 3.15 mmol). The reaction was heated at 90 °C overnight. After cooling, the mixture was diluted with water and extracted with EtOAc. The organic phase was

dried over MgSO₄ and filtered. After evaporation, the crude product was recrystallized from 2-propanol; crystals were collected and dried under vacuum to afford **8k** (62 mg, 6.9% yield), mp: 161–163 °C. ¹H NMR (CDCl₃): δ = 9.01 (1H, dd, *J* = 0.8, 2.3 Hz), 8.53 (1H, dd, *J* = 1.7, 4.8 Hz), 8.12 (1H, ddd, *J* = 1.8, 2.2, 8.0 Hz), 7.94 (1H, d, *J* = 1.3 Hz), 7.58 (1H, d, *J* = 1.3 Hz), 7.34 (1H, ddd, *J* = 0.8, 4.9, 8.0 Hz), 3.95 (1H, m), 3.01 (3H, s), 1.87 (4H, m), 1.71 (1H, d br, *J* = 13.5 Hz), 1.59 (2H, dq, *J* = 3.5, 12.5 Hz), 1.38 (2H, t q, *J* = 3.5, 13.0 Hz), 1.13 ppm (1H, tq, *J* = 3.5, 13.5 Hz); ¹³C NMR (CDCl₃): δ = 151, 148.5, 146.7, 139.2, 137.3, 132.4, 129, 123.6, 114, 57.6, 31.4, 30, 25.4, 25.2 ppm; Elemental analysis calcd (%) for (C₁₆H₂₀N₄O): C 67.58, H 7.09, N 19.7, found: C 66.77, H 7.36, N 19.95.

3-(1-(Cyclohexyl(methyl)carbamoil)-1*H*-imidazol-4-yl)pyridine 1-oxide (8l). To a stirred solution of *N*-cyclohexyl-*N*-methyl-4-(pyridin-3-yl)-1*H*-imidazole-1-carboxamide **8k** (90 mg, 0.317 mmol) was added *m*CPBA (149 mg, 0.475 mmol) at 20–25 °C in one portion. The reaction was allowed to stir at 20–25 °C for 20 h. The mixture was evaporated to dryness, the residue was then triturated in Et₂O. The resulting white crystals were collected, dried on air and recrystallized from isopropanol to afford **8l** (46 mg, 48% yield), mp: 227.5 °C. ¹H NMR ([D₆]DMSO): δ = 8.70 (1H, t, *J* = 1.5 Hz), 8.28 (1H, s), 8.20 (1H, s), 8.11 (1H, d, *J* = 6.5 Hz), 7.78 (1H, d, *J* = 8.1 Hz), 7.45 (1H, dd, *J* = 6.5, 8.1 Hz), 3.80 (1H, m), 2.92 (3H, s), 1.77 (4H, m), 1.56 (3H, m), 1.30 (2H, m), 1.11 ppm (1H, m); ¹³C NMR ([D₆]DMSO): δ = DMSO: 150.4, 138.3, 137.1, 135.7, 134.7, 132.8, 126.7, 121.2, 117, 56.8, 31.4, 29, 25.1, 24.8 ppm; Elemental analysis calcd (%) for (C₁₆H₂₀N₄O₂): C 63.98, H 6.71, N 18.65, found: C 63.76, H 6.94, N 18.74.

(4,4-Dimethyloxazolidin-3-yl)(4-phenyl-1*H*-imidazol-1-yl)methanone (8f). To a stirred solution of 4-phenyl-1*H*-imidazole **9b** (433 mg, 3.00 mmol) in THF (10 mL) at 0 °C was added dropwise a solution of 4,4-dimethyloxazolidine-3-carbonyl chloride (515 mg, 3.15 mmol) in THF (10 mL) followed by pyridine (0.48 mL, 5.93 mmol). The reaction was allowed to stir at room temperature for 1 h, then heated at reflux for 4 h. The mixture was cooled to room temperature and evaporated. The residue was partitioned between CH₂Cl₂ and water. The organic phase was separated, washed with 2*N* HCl, water and brine, then dried over MgSO₄, filtered and evaporated in vacuum. Column chromatography (petroleum ether/EtOAc, 2:1) followed by recrystallization from isopropanol afforded the title compound as a white powder (120 mg, 14%), mp: 89 °C. ¹H NMR (CDCl₃): δ = 7.96 (1H, d, *J* = 1.3 Hz), 7.79 (2H, m, *J* = 8.3 Hz), 7.52 (1H, d, *J* = 1.3 Hz), 7.41 (2H, m, *J* = 7.9 Hz), 7.30 (1H, m, *J* = 7.3 Hz), 5.13 (2H, s), 3.88 (2H, s), 1.62 ppm (6H, s); ¹³C NMR (CDCl₃): δ = 146.5, 142.6, 136.2, 132.7, 128.7, 127.7, 125.2, 112, 81.1, 80.3, 61.8, 22.8 ppm; Elemental analysis calcd (%) for (C₁₅H₁₇N₃O₂): C 66.40, H 6.32, N 15.49, found: C 65.59, H 6.35, N 15.32.

***N*-(2,4-Difluorophenyl)-*N*-methyl-1*H*-benzo[d][1,2,3]triazole-1-carboxamide (10b).** To a stirred solution of phosgene (15 mL, 28.5 mmol, 20% solution in toluene) at 0 °C was added a solution of 1*H*-benzo[d][1,2,3]triazole **9a** (1 g, 8.39 mmol) in THF (20 mL) dropwise. The resulting mixture was stirred in the cold for 0.5 h, then allowed to stir at room temperature overnight. A strong stream of nitrogen was bubbled through the mixture for 0.5 h, then the solvent was removed by evaporation under reduced pressure to give the intermediate 1*H*-benzo[d][1,2,3]triazole-1-carbonyl chloride as a clear oil that solidified on standing (762 mg, 4.2 mmol). The above intermediate was suspended in THF (20 mL), cooled to 0 °C and treated with pyridine (0.36 mL, 4.41 mmol) followed by dropwise addition of 2,4-difluoro-*N*-methylaniline (601 mg, 4.20 mmol). The reaction mixture was allowed to stir at

room temperature overnight, then cooled to 0 °C, diluted with water and EtOAc. The organic layer was separated, washed with 1 N HCl and brine, then dried over MgSO₄ filtered and evaporated. Recrystallization from isopropanol gave **10b** as a white solid (378 mg, 31%), mp: 91–92 °C. ¹H NMR (CDCl₃): δ = 8.10 (1H, d, *J* = 8.4 Hz), 8.01 (1H, d, *J* = 8.1 Hz), 7.63 (1H, m, *J* = 7.8 Hz), 7.45 (1H, t, *J* = 7.7 Hz), 7.30 (1H, m), 6.88 (1H, m), 6.84 (1H, m), 3.60 ppm (3H, s); ¹³C NMR (CDCl₃): δ = 161.8 (dd, *J* = 11.5, 251.0 Hz), 157.7 (dd, *J* = 12.5, 252.0 Hz), 150.1, 144.9, 132.7, 129.6, 129.3 (dd, *J* = 1.5, 10.0 Hz), 127.7 (dd, *J* = 5.0, 12.0 Hz), 125.4, 119.9, 113.5, 112.1 (dd, *J* = 4.0, 23.0 Hz), 105.1 (dd, *J* = 24.0, 26.5 Hz), 39.7 ppm; Elemental analysis calcd (%) for (C₁₄H₁₀F₂N₄O) C, 58.33, H 3.5, N 19.44, found: C 58.66, H 3.52, N 19.75.

***N*-(2,4-Difluorophenyl)-1*H*-benzo[d][1,2,3]triazole-1-carboxamide (10d)**. To an ice-cooled stirred solution of benzotriazole **9a** (300 mg, 2.52 mmol) in CH₂Cl₂ (18 mL) was added 2,4-difluoro-1-isocyanatobenzene (410 mg, 2.64 mmol) dropwise. After being stirred for 6 h at room temperature the solvent was evaporated. Recrystallization from a mixture of isopropanol/CH₂Cl₂ afforded **10d** as a white solid (209 mg, 30%), mp: 148–150 °C. ¹H NMR (CDCl₃): δ = 9.28 (1H, s), 8.32 (1H, m, *J* = 8.3 Hz), 8.27 (1H, m, *J* = 6.0, 8.9 Hz), 8.17 (1H, m, *J* = 8.3 Hz), 7.70 (1H, m, *J* = 8.2 Hz), 7.53 (1H, m, *J* = 8.1 Hz), 7.0 ppm (2H, m); ¹³C NMR (CDCl₃): δ = 160.6 (dd, *J* = 11.5, 248.0 Hz), 153.4 (dd, *J* = 12.0, 249.0 Hz), 146.5, 146.4, 131.5, 130.5, 125.9, 122.7 (dd, *J* = 2.0, 9.3 Hz), 121.0 (dd, *J* = 3.7, 11.0 Hz), 120.4, 113.8, 111.6 (dd, *J* = 4.0, 22.5 Hz), 104.2 ppm (dd, *J* = 22.5, 27.0 Hz); Elemental analysis calcd (%) for (C₁₃H₈F₂N₄O) C, 56.94, H 2.94, N 20.43, found: C 56.86, H 3.09, N 20.73.

1-(4,4-Dimethyloxazolidine-3-carbonyl)-1*H*-benzo[d][1,2,3]triazole-5-carboxylic acid (10p). To an ice-cooled stirred suspension of sodium hydride (7.66 g, 192 mmol) in THF (100 mL) was added a solution of 1*H*-benzo[d][1,2,3]triazole-5-carboxylic acid **9b** (12.5 g, 77 mmol) in a mixture of THF (280 mL) and DMF (160 mL) dropwise. The suspension was allowed to stir at room temperature for 0.5 h followed by dropwise addition of 4,4-dimethyloxazolidine-3-carbonyl chloride (13.16 g, 80 mmol) in THF (50 mL) at 0 °C. The reaction mixture was allowed to stir at room temperature for 5 h. Thereupon, water was carefully added at 0 °C, the THF was evaporated, then 2 N HCl was added until pH 2 was reached. The resulting acidic aqueous phase was extracted three times with a mixture of CH₂Cl₂/isopropanol (7:3). The combined organic layers were dried over MgSO₄ and evaporated. The obtained mobile liquid was azeotroped with toluene to leave a brown oil. Purification by column chromatography in a mixture of CH₂Cl₂/methanol (95:5) afforded **10p** as a beige solid (1.8 g, 34%). ¹H NMR ([D₆]DMSO): δ = 8.71 (1H, dd, *J* = 0.8, 1.3 Hz), 8.26 (1H, sbr), 8.21 (1H, d, *J* = 1.3, 8.6 Hz), 8.16 (1H, dd, *J* = 0.8, 8.6 Hz), 7.63 (1H, sbr), 5.43 (2H, s), 3.90 (2H, s), 1.58 ppm (6H, s); ¹³C NMR ([D₆]DMSO): δ = 166.9, 145.4, 144.6, 133.7, 131.9, 129.1, 119, 113.9, 81.7, 78.7, 61.7, 22.5 ppm.

(6-Bromo-1*H*-benzo[d][1,2,3]triazol-1-yl)(4,4-dimethyloxazolidin-3-yl)methanone (11b). Compound **11b** was prepared by reaction of 6-bromo-1*H*-benzo[d][1,2,3]triazole-1-carbonyl chloride (2.63 g, 10.10 mmol) with 4,4-dimethyloxazolidine (1.5 mL, 10.60 mmol, 75% solution in water) as described for **10b**. Recrystallization from ethanol afforded the title product as a beige solid (253 mg, 7.7%), mp: 119–121 °C. ¹H NMR (CDCl₃): δ = 8.48 (1H, sbr), 7.96 (1H, d, *J* = 8.7 Hz), 7.59 (1H, dd, *J* = 1.5, 8.7 Hz), 5.53 (2H, s), 3.90 (2H, s), 1.68 ppm (6H, s); ¹³C NMR (CDCl₃): δ = 145.7, 144.1, 133.7, 129.3, 124.2, 120.8, 117.5, 82.4, 79.5, 62.4, 22.9 ppm; Elemental analysis calcd (%) for (C₁₂H₁₃BrN₄O₂) C, 44.33, H 4.03, N 17.23, found: C 44.08, H 4.05, N 17.21.

(4,4-Dimethyloxazolidin-3-yl)(6-phenyl-1*H*-benzo[d][1,2,3]triazol-1-yl)methanone (11d). To a stirred suspension of 6-bromo-1*H*-benzo[d][1,2,3]triazol-1-yl)(4,4-dimethyloxazolidin-3-yl)methanone **11b** (0.300 g, 0.92 mmol), phenylboronic acid (0.12 g, 0.97 mmol) and sodium carbonate (0.55 mL, 1.11 mmol) in a mixture of 1-propanol (3.4 mL) and water (0.7 mL) at room temperature was added tetrakis(triphenylphosphine)palladium(0) (53 mg, 0.046 mmol). The resulting yellow mixture was stirred at 90 °C for 2 h, then cooled to room temperature and a second crop of tetrakis(triphenylphosphine)palladium(0) (20 mg, 0.16 mmol) was added. The reaction mixture was allowed to stir for a further 2 h at 90 °C. After cooling to room temperature, the solvent was removed under reduced pressure. The residue was dissolved in EtOAc and the organic phase was washed with water. The organic phase was dried over MgSO₄, filtered, and evaporated to leave a yellow oil. Purification by column chromatography in a mixture of (petroleum ether/EtOAc, 20:1) followed by recrystallization from isopropanol afforded the title compound **11d** as a white solid (72 mg, 24%), mp: 146–147 °C. ¹H NMR (CDCl₃): δ = 8.44 (1H, dd, *J* = 1.7, 1.6 Hz), 8.14 (1H, dd, *J* = 0.7, 8.7 Hz), 7.74 (1H, dd, *J* = 1.6, 8.7 Hz), 7.71 (2H, m, *J* = 8.2 Hz), 7.50 (2H, m, *J* = 7.9 Hz), 7.42 (1H, m, *J* = 7.5 Hz), 5.57 (2H, s), 3.92 (2H, s), 1.70 ppm (6H, s); ¹³C NMR (CDCl₃): δ = 146.2, 144.7, 143.1, 140.2, 133.5, 128.9, 128.1, 127.9, 125.7, 119.9, 112.4, 82.5, 79.6, 62.2, 23 ppm; Elemental analysis calcd (%) for (C₁₈H₁₈N₄O₂) C, 67.07, H 5.63, N 17.38, found: C 66.92, H 5.62, N 17.67.

1-(4,4-Dimethyloxazolidine-3-carbonyl)-1*H*-benzo[d][1,2,3]triazole-5-carboxamide (11h). To a stirred solution of 1-(4,4-dimethyloxazolidine-3-carbonyl)-1*H*-benzo[d][1,2,3]triazole-6-carboxylic acid **10p** (0.76 g, 2.63 mmol) and pyridine (0.70 mL, 8.67 mmol) in CH₂Cl₂ (17 mL) was added thionyl chloride (0.63 mL, 8.67 mmol) dropwise at room temperature. The obtained yellow solution was allowed to stir at room temperature for 15 min followed by dropwise addition to a 1.75 M ethanolic solution of ammonia (15 mL, 26.3 mmol) at 0 °C. The reaction mixture was stirred at room temperature for 0.5 h. Thereupon, water was added and the ethanol was evaporated under reduced pressure. The resulting aqueous phase was extracted with CH₂Cl₂. The organic layer was separated, washed with 1 N HCl, then dried over MgSO₄ filtered and evaporated. Recrystallization from a mixture of CH₂Cl₂/ethanol afforded **11h** as a beige solid (151 mg, 20%), mp: 216–218 °C. ¹H NMR ([D₆]DMSO): δ = 8.71 (1H, dd, *J* = 0.8, 1.3 Hz), 8.26 (1H, sbr), 8.21 (1H, d, *J* = 1.3, 8.6 Hz), 8.16 (1H, dd, *J* = 0.8, 8.6 Hz), 7.63 (1H, sbr), 5.43 (2H, s), 3.90 (2H, s), 1.58 ppm (6H, s); ¹³C NMR ([D₆]DMSO): δ = 166.9, 145.4, 144.6, 133.7, 131.9, 129.1, 119, 113.9, 81.7, 78.7, 61.7, 22.5 ppm; Elemental analysis calcd (%) for (C₁₃H₁₅N₅O₃) C, 53.97, H 5.23, N 24.21, found: C 53.65, H 5.51, N 24.54.

Pharmacology

Animal treatment: All animal procedures conformed to the guidelines from Directive 2010/63/EU of the European Parliament on the protection of animals used for scientific purposes and the Portuguese law on animal welfare (Decreto-Lei 113/2013). Adult male NMRI mice were obtained from Harlan (Spain). Animals were maintained in macrolon cages (Tecniplast, Italy) with free access to food (2014 Teklad Global 14% Protein Rodent Maintenance, Envigo) and tap water under controlled environmental conditions in a colony room (12 hour light/dark cycle, room temperature: 22 ± 2 °C and relative humidity: 60 ± 10%). Experiments were carried out during daylight hours. Animals were then given just water. Overnight-fasted animals were administered compounds via oral route (gavage) at 8 mL kg⁻¹ using animal feeding stainless steel needles (Perfectum, USA). For the 24 h time point the food was removed in

the morning of the day of administration and compounds administered at the end of the afternoon of the same day. For ED₅₀ determination doses administered were 0.001, 0.003, 0.01, 0.03, and 0.1 mg kg⁻¹ in 10% (v/v) DMSO. The vehicle for other compound administrations was 0.5% (w/v) carboxymethylcellulose except for compound **2** that was 5% *N,N*-dimethylacetamide and 95% 2-hydroxypropyl- β -cyclodextrin (40% w/v in water). Fifteen minutes before sacrifice animals were anesthetized with 60 mg kg⁻¹ pentobarbital sodium administered intraperitoneally. A fragment of liver and brain without cerebellum were removed and put in plastic vials containing membrane buffer (3 mM MgCl₂, 1 mM EDTA, 50 mM Tris-HCl pH 7.4). Tissues were stored at -30 °C until processed for analysis where tissues were thawed on ice and were homogenized in 10 volumes of membrane buffer with Heidolph Diax (position 5, 30 s for livers and 20 s for brains). FAAH activity was evaluated in these preparations.

Reagents and solutions: Tritiated anandamide [ethanolamine-1-³H] ([³H]AEA, 40–60 Ci mmol⁻¹) and 2-monoleoyl glycerol ([³H]2-OG, 40–60 Ci mmol⁻¹) were obtained from American Radiochemicals (USA). 1-Oleoyl-*rac*-glycerol (OG), arachidonylethanolamide (AEA), fatty acid free bovine serum albumin (BSA), and all other reagents were obtained from Merck (Germany). Optiphase Supermix was obtained from PerkinElmer (USA).

Enzyme assays: FAAH activity in vitro and in tissues preparations from treated animals was evaluated essentially as described by Kiss et al.^[44] In brief, for compound evaluation in vitro reaction mix (total volume of 200 μ L) contained: 2 μ M AEA (2 μ M AEA + 5 nM [³H]AEA), 0.1% fatty acid free BSA, 5 μ g rat brain membrane preparation and the compound to evaluate in 1 mM EDTA, 10 mM Tris pH 7.6. After a 15 min pre-incubation period at 37 °C, reaction was started by the addition of the substrate solution (cold AEA + radio-labeled AEA + BSA). Reaction was carried out for 10 min before termination. For tissues from treated animals the reaction contained 15 μ g (brain) or 5 μ g (liver) protein, no compound, and after a pre-incubation period of 10 min reaction was carried out for 10 min (brain) or 7 min (liver) before termination. Reactions were terminated by the addition of 400 μ L activated charcoal suspension (8 g charcoal in 32 mL 0.5 M HCl in continuous agitation). After a 30 min incubation period at room temperature with agitation, charcoal was sedimented by centrifugation in a microfuge (10 min at 13000 rpm); 200 μ L of the supernatant were added to 800 μ L Optiphase Supermix scintillation cocktail previously distributed in 24-well plates. Counts per minute (cpm) were determined in a MicrobetaTriLux scintillation counter (PerkinElmer). In each assay, blanks (without protein) were prepared. The percentage of remaining enzymatic activity was calculated with respect to controls (no compound) and after blank subtraction. In some assays reaction was terminated by the addition of 400 μ L chloroform/methanol (1:1 v/v). Reactions were vortexed twice, left on ice for 5 min and were then centrifuged in microfuge (7 min at 7000 rpm). Counts per minute were determined in 200 μ L of the supernatant as described above.

MAGL assay: MAGL activity was determined using cerebellar cytosol prepared from Wistar rats. In brief, cerebella were homogenized at 4 °C in sodium phosphate buffer (50 mM, pH 8) containing 0.32 M sucrose. Homogenates were then centrifuged at 100000 g for 60 min at 4 °C. The supernatants (cytosol fractions) were collected and stored frozen in aliquots at -70 °C until used for assay. Reaction contained, in a final volume of 200 μ L, 100 μ M test compound, 8 μ g total protein, the substrate (2 μ M 1-oleoyl-*rac*-glycerol and 5 nM [³H]2-OG), 0.1% fatty acid free BSA in 1 mM EDTA 10 mM Tris-HCl, pH 7.2. Reaction was started with substrate after a 10 min

pre-incubation period and was carried out for 8 min at 37 °C until termination with 400 μ L chloroform/methanol (1:1 v/v). Phase separation was achieved by microfuge centrifugation (7 min, 7000 rpm); 200 μ L of the methanol phase were added to 800 μ L Optiphase Supermix scintillation cocktail previously distributed in 24-well plates. Counts per minute (cpm) were determined in a MicrobetaTriLux scintillation counter (PerkinElmer). In each assay blanks (without protein) were prepared. The percentage of remaining enzymatic activity was calculated with respect to controls (no compound) and after blank subtraction. Total protein was determined with a Bio-Rad Protein Assay kit using a standard curve of BSA (50–250 mg mL⁻¹).

CE activity determination: The assay to evaluate the CE activity was conducted in 96-well plates at 37 °C using a modified method described by Wheelock et al.^[45] Briefly, rat liver microsomes (8 μ g mL⁻¹) were incubated for 15 min in a shaking water bath in the presence or absence of 10 μ M test compounds, in a final volume of 100 μ L. Test compounds stock solutions (10 mM) were initially dissolved in DMSO, but the final concentration of the solvent in the reaction medium was kept below 0.1%, which had no effect on CE activity. After 15 min incubation, the enzymatic reaction was initiated by the addition of 1 mM 4-nitrophenyl acetate (prepared in ethanol with less than 0.5% in final solution). Incubation occurred for 10 min in a shaking water bath at 37 °C. The reaction was stopped by adding acetonitrile and the CE activity was measured at 405 nm using a spectrophotometer. The CE activity without test compounds was set at 100% and the remaining CE activity after incubation with test compounds was calculated relative to the control. All experiments were performed with samples in quadruplicate.

CYP450 metabolic stability assay: Stability of the test compounds was performed in liver microsomes in the presence and absence of NADPH. The stability was measured using the incubation mixture (100 μ L total volume) containing 1 mg mL⁻¹ total protein, 5 mM MgCl₂, and 50 mM potassium phosphate buffer. Samples were incubated in the presence and absence of NADPH (1 mM). Reactions were pre-incubated for 5 min and the reaction was initiated with addition of the test compound (5 μ M for human liver microsomes and 50 μ M for mouse liver microsomes). Samples were incubated for 60 min in a shaking water bath at 37 °C. The reaction was stopped by adding 100 μ L of acetonitrile. Samples were then centrifuged, filtered, and supernatant injected in HPLC-MSD. Test compounds were dissolved in DMSO and the final concentration of DMSO in the reaction was below 0.5% (v/v). At *t*₀ acetonitrile was added before adding the compound. All experiments were performed with samples in duplicate.

Conflict of interest

The authors declare no conflict of interest.

Keywords: anandamide · BIA 10-2474 · fatty acid amide hydrolase · pain · target selectivity

- [1] M. K. McKinney, B. F. Cravatt, *Annu. Rev. Biochem.* **2005**, *74*, 411–432.
- [2] B. F. Cravatt, D. K. Giang, S. P. Mayfield, D. L. Boger, R. A. Lerner, N. B. Gilula, *Nature* **1996**, *384*, 83–87.
- [3] D. M. Lambert, C. J. Fowler, *J. Med. Chem.* **2005**, *48*, 5059–5087.
- [4] B. F. Cravatt, A. H. Lichtman, *Curr. Opin. Chem. Biol.* **2003**, *7*, 469–475.
- [5] W. Tuo, N. Leleu-Chavain, J. Spencer, S. Sansook, R. Millet, P. Chavatte, *J. Med. Chem.* **2017**, *60*, 4–46.

- [6] K. Ahn, M. K. McKinney, B. F. Cravatt, *Chem. Rev.* **2008**, *108*, 1687–1707.
- [7] S. Vandevoorde, *Curr. Top. Med. Chem.* **2008**, *8*, 247–267.
- [8] K. Ahn, D. S. Johnson, B. F. Cravatt, *Expert Opin. Drug Discovery* **2009**, *4*, 763–784.
- [9] H. Deng, *Expert Opin. Drug Discovery* **2010**, *5*, 961–993.
- [10] A. Lodola, R. Castelli, M. Mor, S. Rivara, *Expert Opin. Ther. Pat.* **2015**, *25*, 1247–1266.
- [11] M. H. Bracey, M. A. Hanson, K. R. Masuda, R. C. Stevens, B. F. Cravatt, *Science* **2002**, *298*, 1793–1796.
- [12] M. Mileni, D. S. Johnson, Z. Wang, D. S. Everdeen, B. Pabst, K. Bhattacharya, R. A. Nugent, S. Kamtekar, B. F. Cravatt, K. Ahn, R. C. Stevens, *Proc. Natl. Acad. Sci. USA* **2008**, *105*, 12820–12824.
- [13] K. Ahn, D. S. Johnson, M. Mileni, D. Beidler, J. Z. Long, M. K. McKinney, E. Weerapana, N. Sadagopan, M. Liimatta, S. E. Smith, S. Lazerwith, C. Stiff, S. Kamtekar, K. Bhattacharya, Y. Zhang, S. Swaney, K. Van Becelaere, R. C. Stevens, B. F. Cravatt, *Chem. Biol.* **2009**, *16*, 411–420.
- [14] M. Mileni, J. Garfunkle, J. K. DeMartino, B. F. Cravatt, D. L. Boger, R. C. Stevens, *J. Am. Chem. Soc.* **2009**, *131*, 10497–10506.
- [15] M. Mileni, J. Garfunkle, C. Ezzili, F. S. Kimball, B. F. Cravatt, R. C. Stevens, D. L. Boger, *J. Med. Chem.* **2010**, *53*, 230–240.
- [16] M. Mileni, S. Kamtekar, D. C. Wood, T. E. Benson, B. F. Cravatt, R. C. Stevens, *J. Mol. Biol.* **2010**, *400*, 743–754.
- [17] C. Ezzili, M. Mileni, N. McGlinchey, J. Z. Long, S. G. Kinsey, D. G. Hochstatter, R. C. Stevens, A. H. Lichtman, B. F. Cravatt, E. J. Bilsky, D. L. Boger, *J. med. Chem.* **2011**, *54*, 2805–2822.
- [18] M. Mileni, J. Garfunkle, C. Ezzili, B. F. Cravatt, R. C. Stevens, D. L. Boger, *J. Am. Chem. Soc.* **2011**, *133*, 4092–4100.
- [19] K. Otrubova, M. Brown, M. S. McCormick, G. W. Han, S. T. O'Neal, B. F. Cravatt, R. C. Stevens, A. H. Lichtman, D. L. Boger, *J. Am. Chem. Soc.* **2013**, *135*, 6289–6299.
- [20] D. L. Boger, H. Miyauchi, W. Du, C. Hardouin, R. A. Fecik, H. Cheng, I. Hwang, M. P. Hedrick, D. Leung, O. Acevedo, C. R. Guimaraes, W. L. Jorgensen, B. F. Cravatt, *J. Med. Chem.* **2005**, *48*, 1849–1856.
- [21] M. Mor, S. Rivara, A. Lodola, P. V. Plazzi, G. Tarzia, A. Duranti, A. Tontini, G. Piersanti, S. Kathuria, D. Piomelli, *J. Med. Chem.* **2004**, *47*, 4998–5008.
- [22] K. Ahn, D. S. Johnson, L. R. Fitzgerald, M. Liimatta, A. Arendse, T. Stevenson, B. F. Cravatt, *Biochemistry* **2007**, *46*, 13019–13030.
- [23] J. M. Keith, R. Apodaca, W. Xiao, M. Seierstad, K. Pattabiraman, J. Wu, M. Webb, M. J. Karbarz, S. Brown, S. Wilson, B. Scott, C. S. Tham, L. Luo, J. Palmer, M. Wennerholm, S. Chaplan, J. G. Breitenbucher, *Bioorg. Med. Chem. Lett.* **2008**, *18*, 4838–4843.
- [24] D. S. Johnson, K. Ahn, S. Kesten, S. E. Lazerwith, Y. Song, M. Morris, L. Fay, T. Gregory, C. Stiff, J. B. Dunbar, Jr., M. Liimatta, D. Beidler, S. Smith, T. K. Nomanbhoy, B. F. Cravatt, *Bioorg. Med. Chem. Lett.* **2009**, *19*, 2865–2869.
- [25] J. M. Keith, W. M. Jones, M. Tichenor, J. Liu, M. Seierstad, J. A. Palmer, M. Webb, M. Karbarz, B. P. Scott, S. J. Wilson, L. Luo, M. L. Wennerholm, L. Chang, M. Rizzolio, R. Rynberg, S. R. Chaplan, J. G. Breitenbucher, *ACS Med. Chem. Lett.* **2015**, *6*, 1204–1208.
- [26] D. S. Johnson, C. Stiff, S. E. Lazerwith, S. R. Kesten, L. K. Fay, M. Morris, D. Beidler, M. B. Liimatta, S. E. Smith, D. T. Dudley, N. Sadagopan, S. N. Bhattachar, S. J. Kesten, T. K. Nomanbhoy, B. F. Cravatt, K. Ahn, *ACS Med. Chem. Lett.* **2011**, *2*, 91–96.
- [27] J. P. Huggins, T. S. Smart, S. Langman, L. Taylor, T. Young, *Pain* **2012**, *153*, 1837–1846.
- [28] H. R. Chobanian, Y. Guo, P. Liu, M. D. Chioda, S. Fung, T. J. Lanza, L. Chang, R. K. Bakshi, J. P. Dellureficio, Q. Hong, M. McLaughlin, K. M. Belyk, S. W. Krska, A. K. Makarewicz, E. J. Martel, J. F. Leone, L. Frey, B. Karanam, M. Madeira, R. Alvaro, J. Shuman, G. Salituro, J. L. Terebetski, N. Jochowitz, S. Mistry, E. McGowan, R. Hajdu, M. Rosenbach, C. Abbadie, J. P. Alexander, L. L. Shiao, K. M. Sullivan, R. P. Nargund, M. J. Wyvrat, L. S. Lin, R. J. DeVita, *ACS Med. Chem. Lett.* **2014**, *5*, 717–721.
- [29] L. E. Kiss, D. A. Learmonth, C. Rosa, R. Noronha, P. N. Palma, P. Soares-da-Silva, A. Beliaev (BIAL-Portela & C^a, S.A.), Int. PCT Pub. No. WO2010074588, **2010**.
- [30] A. Makriyannis, L. Pandarinathan, N. Zvonok, T. Parkkari, L. Chapman (Northeastern University, Boston, USA) Int. PCT Pub. No. WO2009117444, **2009**.
- [31] J. L. G. Nilsson, H. Sievertsson, R. Dahlbom, *Acta Chem. Scand.* **1968**, *22*, 683–685.
- [32] L. Boldrup, S. J. Wilson, A. J. Barbier, C. J. Fowler, *J. Biochem. Biophys. Methods* **2004**, *60*, 171–177.
- [33] D. Piomelli, G. Tarzia, A. Duranti, A. Tontini, M. Mor, T. R. Compton, O. Dasse, E. P. Monaghan, J. A. Parrott, D. Putman, *CNS Drug Rev.* **2006**, *12*, 21–38.
- [34] D. Russo, G. B. R. Whanon, W. Maton, T. Eszenyi, (BIAL-Portela & C^a, S.A.), Int. PCT Pub. No. WO2014017938, **2014**.
- [35] A. Kerbrat, J. C. Ferre, P. Fillatre, T. Ronziere, S. Vannier, B. Carsin-Nicol, S. Lavoue, M. Verin, J. Y. Gauvrit, Y. Le Tulzo, G. Edan, *N. Engl. J. Med.* **2016**, *375*, 1717–1725.
- [36] CSST (2016), *Report by the Temporary Specialist Scientific Committee (TSSC): "FAAH (Fatty Acid Amide Hydrolase)", on the causes of the accident during a Phase 1 clinical trial in Rennes in January 2016*, http://ansm.sante.fr/var/ansm_site/storage/original/application/744c7c6daf96b141bc9509e2f85c227e.pdf (accessed August 31, 2018).
- [37] A. C. M. van Esbroeck, A. P. A. Janssen, A. B. Cognetta III, D. Ogasawara, G. Shpak, M. van der Kroeg, V. Kantae, M. P. Baggelaar, F. M. S. de Vrij, H. Deng, M. Allarà, F. Fezza, Z. Lin, T. van der Wel, M. Soethoudt, E. D. Mock, H. den Dulk, I. L. Baak, B. I. Florea, G. Hendriks, L. De Petrocellis, H. S. Overkleeft, T. Hankemeier, C. I. De Zeeuw, V. Di Marzo, M. Maccarone, B. F. Cravatt, S. A. Kushner, M. van der Stelt, *Science* **2017**, *356*, 1084–1087.
- [38] R. J. Richardson, N. D. Hein, S. J. Wijeyesakere, J. K. Fink, G. F. Makhaeva, *Chem.-Biol. Interact.* **2013**, *203*, 238–244.
- [39] M. J. Bonifácio, C. Lopes, N. Pires, A. I. Loureiro, P. Moser, P. Soares-da-Silva, *pA₂ online* **2017**, *16*, 203P.
- [40] A. I. Loureiro, C. Lopes, M. J. Bonifácio, P. Moser, P. Soares-da-Silva, *pA₂ online* **2017**, *16*, 216P.
- [41] A. I. Loureiro, C. Lopes, M. J. Bonifácio, P. Moser, P. Soares-da-Silva, *pA₂ online* **2017**, *16*, 212P.
- [42] J. F. Rocha, A. Santos, D. Chassard, A. Patat, A. Astruc, A. Falcão, H. Gama, P. Soares-da-Silva, *pA₂ online* **2017**, *16*, 178P.
- [43] H. Gama, M. Vieira, J. Graça, D. Chassard, J. Massano, H. Charfi, A. Patat, A. Santos, J. F. Rocha, P. Soares-da-Silva, *pA₂ online* **2017**, *16*, 188P.
- [44] L. E. Kiss, H. S. Ferreira, A. Beliaev, L. Torrão, M. J. Bonifácio, D. A. Learmonth, *Med. Chem. Commun.* **2011**, *2*, 889–894.
- [45] C. E. Wheelock, T. F. Severson, B. D. Hammock, *Chem. Res. Toxicol.* **2001**, *14*, 1563–1572.

Manuscript received: June 11, 2018

Revised manuscript received: July 27, 2018

Accepted manuscript online: August 16, 2018

Version of record online: September 11, 2018